ANYAGVIZSGÁLÓK LAPJA
MINŐSÉGBIZTOSÍTÁS * ÁLLAPOTELLENŐRZÉS
Elektronikus folyóirat
2010/1-2

Kord-gumi kompozitok mechanikai tulajdonságának mérése
Measurements of mechanical properties of cord-rubber composites

I. Petrikova - B. Marvalova - L. Prasil

Kulcsszavak: kord-gumi kompozitok, mechanikai tulajdonságok, nagymértékű deformáció, fenomenológiai modell
Key words: cord-rubber composites, mechanical properties, large deformations, *phenomenological model*

Összefoglalás

Egy olyan fenomenológiai modellt dolgoztak ki, amely alkalmas a gumi mátrixú, kord szálakkal erősített kompozit anyagok nagymértékű deformációjának kiszámítására. Az izotóp gumi mátrix viselkedése az új Hooke, a Mooney_Rivlin vagy az Ogden modellekkel, és a beágyazott kord szálak hatása pedig polinom vagy exponenciális függvényekkel írható le, amelyekben a tenzor függ a kord szálak irányától. A jelenséget leíró modell paraméterei a kísérleti eredményekből határozható meg. Különböző optikai módszereket, úgy mint képfeldolgozást és a digitális képek korrelációját használták az elmozdulások mérésére.

Abstract

A phenomenological constitutive model that is capable of predicting the large deformations of cord composites with rubber matrix has been developed. The behavior of the isotropic rubber matrix was described by neo-Hookean, Mooney-Rivlin or Ogden models and the anisotropic influence of the cords was embodied by the exponential or polynomial functions of structural tensors depending on cord directions. Parameters of constitutive model were determined from experimental measurements. Different optical methods such as the image processing and the digital image correlation were used for the displacement measurements.

Introduction

Our intensive experimental and theoretical research of cord-rubber composites is part of a broader program, which focuses on the behavior of air-springs. An air-spring shell is an example of layered multiphase flexible composite structure that consists of rubber matrix and stiff reinforcement made of textile cords. The high-modulus, low-elongation cords carry most of the load, and the low-modulus, high-elongation rubber matrix preserves the integrity of the composite and distributes the load. The primary objective of this type composite is to withstand large deformation and cyclic loading while providing high-load carrying capacity. The measurements of displacements and deformations have always been an important topic in the evaluation of material properties such as material strengths or fracture parameters as well as in experimental stress analysis. Optical techniques such as moiré interferometry, holography and speckle interferometry proved to be suitable techniques of deformation analysis are used successfully in many different applications. However, each method has specific disadvantages that limit its use. In the last decade, a non-contacting optical technique, digital image correlation (DIC), has been introduced, whose basic principles are well described in several papers, e.g. Lyons (1996), Garcia (2002) and references mentioned therein. The DIC technique offers qualitative and quantitative information on the object heterogeneous deformation. The displacements of the object under test are inferred by tracking changes of a random speckle pattern dashed at the object surface. Tangential displacements and strains at the object surface are calculated based on a comparison between subsequent digital images acquired during loading. The displacement resolution is typically of sub-pixel accuracy and the maximum strain accuracy is in the order of 0.02%. When installed perpendicular to a flat object, only one CCD camera is sufficient to determine in-plane deformations and strains. However, the obtained displacement field is only reliable under the assumption that out-of-plane deformation can be neglected. In order to measure three-dimensional displacements and deformations of arbitrary objects, a binocular stereo-correlation based technique has been developed. The simultaneous observation of the object from different directions allows the 3D movement of each object point to be determined. Image correlation techniques have proven to be a flexible and useful tool for deformation analysis and several complex measuring DIC systems are already commercially available.

Modelling of cord-rubber composites

Common applications of cord-rubber composites include pneumatic tires, air springs, hoses, sleeves, couplings, belts, bladders, diaphragms, and various membrane structures. The cords have

Technical University of Liberec Czech Republic

high axial stiffness and high axial strength, as well as small bending stiffness and long fatigue life. The matrix separates and protects the cords, and it can sustain large strains and resist wear. In addition, the matrix provides a web between the cords to carry or contain loose material, such as gravel on a conveyer belt, or to contain liquids or gases inside such structures such as bladders, tanks, hoses, tires, air springs, and diaphragms.

The reinforcement of thin-walled "rubber bellows" of air-spring is made up of two families of textile cords distributed symetrically with respect to the axis of air-spring, see Fig.1. Owing to this configuration and to the manner of the loading by inner pressure, the material behaves like orthotropic with axes of symmetry in axial and circumferential directions respectively. We assume the isochoric deformation and neglect the dissipation due to irreversible effects. Thus the material is considered as hyperelastic incompressible locally-orthotropic composite.

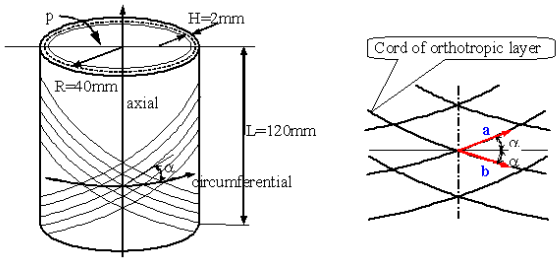

Fig.1. Cord reinforcement distribution
1. ábra Erősítő kord szálak eloszlása

A phenomenological constitutive model that is capable of predicting the large deformations of composites with rubber matrix reinforced by cords has been presented by Marvalova & Urban (2001). The behavior of the rubber matrix was described by Ogden model and the influence of the cords was embodied by the exponential function that was proposed by Holzapfel (2000) and applied to the finite strain calculation of a fiber reinforced rubber tube. The strain energy function of the orthotropic hyperelastic material can be supposed as the sum of the energy stored in matrix material (isotropic part defined by Ogden model) and in cords (anisotropic part depending on the cord elongation)

$$\Psi(\lambda_1,\lambda_2)=\sum_{i=1}^{3}\frac{\mu_i}{\alpha_i}\left(\lambda_1^{\alpha_i}+\lambda_2^{\alpha_i}+\lambda_1^{-\alpha_i}\lambda_2^{-\alpha_i}-3\right)+\frac{k_1}{k_2}\left\{\exp[k_2(\lambda_2^2\cos^2\alpha+\lambda_1^2\sin^2\alpha-1)^2]-1\right\}, \quad (1)$$

where λ1 and λ2 are the stretches in circumferential and axial directions, and α is the angle of the two families of reinforcing fibers. The parameters μ_i,α_i,k_1,k_2 have to be determined from experimental measurements.

Experimental part

Generally, experimental testing under biaxial loading is the appropriate approach for properly evaluating and understanding the material behavior under complex stress states. However, the 2-D state of stress rises in pneumatic membranes that are commonly used for biaxial or equibiaxial loading in material tests. Hence, our experimental measurements were conducted on the air-springs in situ and a testing methodology was designed allowing the stress–stretch behavior of inflated cylindrical air-spring shell to be defined for accurate prediction of material parameters.

The process of determining the material properties involves:

- inflating a tubular specimen – a cylindrical air-spring,
- measuring the principal strains and the geometry of deformed specimen shape by digital image processing
- analytical determining values of stress components based on the theory of nonlinear membranes Green & Adkins (1965)
- determining of the material parameters by nonlinear optimization methods
- using computer simulation to verify and refine the determined values of material parameters

Determination of stress in cylindrical orthotropic membrane

The thin cylindrical membrane at Fig. 2 has the initial radius of mid-surface R, and length 2L. Its initial wall thickness H is assumed to be uniform. The undeformed shape of membrane is described by the polar coordinate system, (X, Φ, R). The cylindrical membrane is inflated by the internal pressure p.

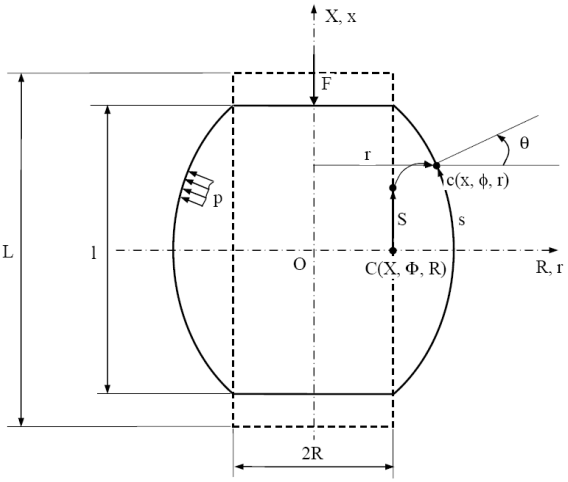

Fig.2. Geometry of cylindrical membrane
2. ábra A hengeres membrán geometriája

The deformed membrane is referred to the polar coordinate system (x, ϕ, r). A material particle moves during the deformation from the position in the undeformed configuration, C(X, Φ, R) to the deformed one, c(x, ϕ, r), along its quasi-equilibrium path. We assume the axisymmetric deformation, e.g. $\phi \equiv \Phi$. We introduce an additional variable θ, the angle of the tangent line. The principal stretches λ1 and λ2 in axial and circumferential directions, principal curvatures κ1 and κ2 and geometric relations are

$$\lambda_1 = \frac{ds}{dS},\ \lambda_2 = \frac{r}{R},\ \frac{dr}{ds} = -\sin\theta,$$
$$\frac{dx}{ds} = \cos\theta,\ \kappa_1 = \frac{d\theta}{ds},\ \kappa_2 = \frac{\cos\theta}{r} \qquad (2)$$

where s is the arc length measured from pole (x = 0) to the particle c(x, ϕ, r) along the meridian of the deformed contour. S is the length corresponding to s on the undeformed contour. The radius r and the thickness h of the membrane are measured with respect to the deformed configuration. The radial stretch λ3 is determined from the incompressibility constraint

$$\lambda_1\lambda_2\lambda_3 = 1 \qquad (3)$$

then

$$h = \frac{H}{\lambda_1\lambda_2} \qquad (4)$$

where R and H are the radius and the thickness respectively in the undeformed configuration. We carried out several series of experiments relating to inflation of cylindrical air-spring with the variable axial force F and the inner pressure. The Cauchy stress is determined based on the equilibrium condition

$$\sigma_1 = \frac{p\pi r^2 - F}{2\pi rh\cos\theta} \qquad (5)$$

Substituting r = λ2R and (4) into (5) we obtain σ_1 as

$$\sigma_1 = A\frac{1}{\cos\theta}\lambda_1\left(\lambda_2^2 - B\right), \qquad (6)$$

where A = $\frac{pR}{2H}$, B = $\frac{F}{\pi pR^2}$. Values of λ1 and λ2 in axial and circumferential directions, the tangent angle θ, as well as principal curvatures κ1 and κ2 are determined from digital image records of deformed membrane. We can deduce σ_2 from the membrane equilibrium equation

$$\kappa_1\sigma_1 + \kappa_2\sigma_2 = \frac{p}{h}. \qquad (7)$$

Constitutive relations – determination of material parameters

The Cauchy stresses are defined as the partial derivatives of appropriate strain energy function Ψ chosen in form (1) with respect to stretches. We have the following expressions:

$$\sigma_1 - \sigma_3 = \lambda_1\frac{\partial\Psi(\lambda_1,\lambda_2)}{\partial\lambda_1},$$
$$\sigma_2 - \sigma_3 = \lambda_2\frac{\partial\Psi(\lambda_1,\lambda_2)}{\partial\lambda_2}, \qquad (8)$$

where $\sigma_3 = -p$, the inner pressure. The experimentally measured values of λ1 and λ2 at several points of the central part of our cylindrical membrane and corresponding stresses were substituted into the equations (8). We get an overdetermined system of nonlinear equations for the parameters $\mu_i, \alpha_i, k_1, k_2$ which were solved in Matlab by nonlinear optimization methods.

Experimental equipment and measurements

The loading of composite membranes and air-springs was realized by means a special loading device at Fig. 3 which enabled the inflation of membrane by pressurized water and in the same time the pressing by the axial force. Several optical measuring systems were built up in our laboratory for an accurate measurement of surface deformations of inflated membranes.

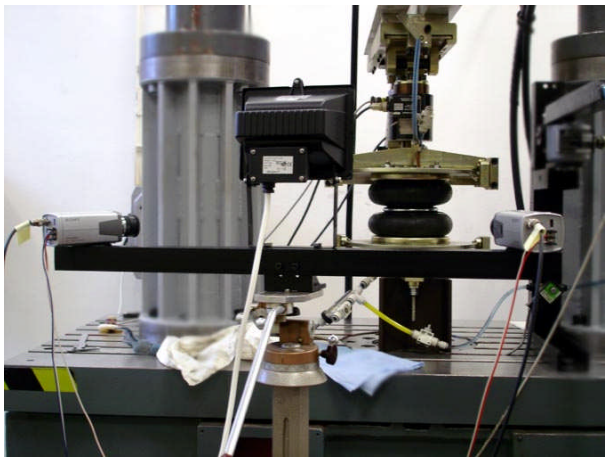

Fig.3. Loading device and optical system with two digital cameras
3. ábra. Terhelő berendezés és a két kamerás optikai rendszer

In the system at Fig. 3 two digital cameras SONY SSC-M383CE are used to acquire digitized b/w images of 768 x 576 pixels. The cameras explored the surface of air-spring shell before and after deformation at different stages of loading and unloading and the data obtained were transmitted to National Instruments IMAQ PCI-1408 card. The axial force and the inner pressure were measured and stored at every stage of loading. The 3D displacements and deformations and also deformed shape of the air-spring surface are measured based on the photographic records using the stereo-correlation technique. For this purpose the software in MATLAB was assembled by the help of toolboxes and techniques explained in Bouguet (2004). The experimental tests were carried out at five different positions of the air-spring. First the end plates of the unloaded air-spring were fixed at the distance by 15, 20, 30, 40 or 50 mm shorter than the free height of the air-spring. Then the air-spring was loaded and unloaded gradually by step 0.05MPa in the range 0.1–0.5MPa. Photographs of the deformed sheet were recorded by the cameras. The principal stretches $\lambda 1$ and $\lambda 2$ in axial and circumferential directions and principal curvatures $\kappa 1$ and $\kappa 2$ were measured from the records.

The experimentally determined material parameters of the air-spring made of so-called balanced angle-ply cord-rubber composite with the angle of fibers α= 48.8o are in Table 1.

Table 1.			
i	1	2	2
μ_i [kPa]	630	1.2	-10
α_i	1.3	5	-2
k_1 [kPa]	4.19 e+04		
k_2	-23.8		

FE simulation of air-spring deformation was carried out based on the constitutive model (1) with the material parameters in Table 1. The experimentally measured stretches and the calculated ones at different points of air-spring are in a good agreement as can be seen at Fig.4.

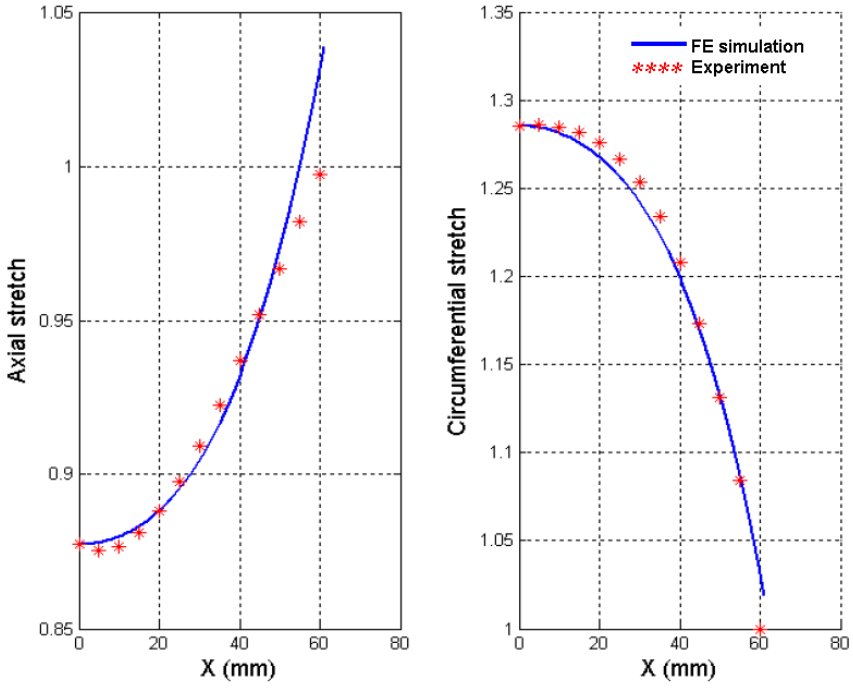

Fig.4. Axial and circumferential stretches at different points of air-spring at the inner pressure of 0.25 MPa
4. ábra: Axiális és érintőleges nyúlások a légrugó különböző pontjaiban 0.25 MPa belső nyomásnál

The equilibrium paths were calculated by FEM in Matlab and the dependency of axial and circumferential stretches on loading inner pressure was determined. Limit points were detected in the following path by using combination of modified Newton-Raphson and arc-length methods. Numerical results obtained correspond to the experimentally measured deformation of the inflated cylindrical air-spring as is shown in Figs. 5 and 6 where stretches at the origin of coordinate system of air-spring (Fig. 2) are illustrated.

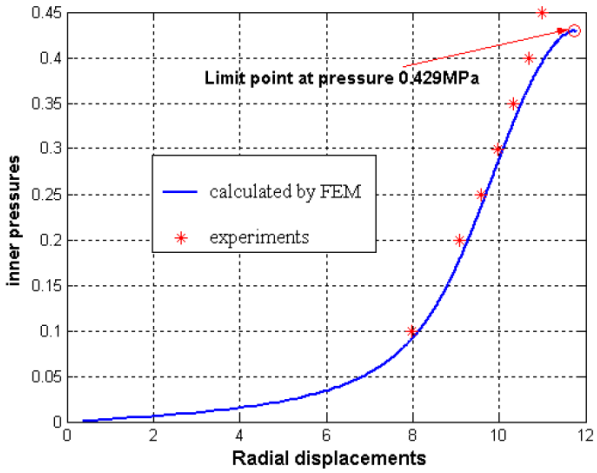

Fig.5. Circumferential stretch as a function of the inner pressure
5. ábra: Érintőleges nyúlások a belső nyomás függvényében

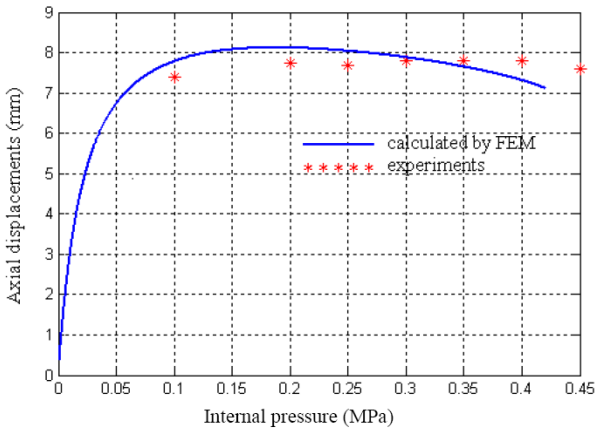

Fig.6. Axial stretch as a function of the inner pressure
6. ábra: Axiális nyúlások a belső nyomás függvényében

Nowadays we use the digital image correlation system Q-400 Dantec Dynamics which is an optical instrument for full-field, non-contact measurement of deformations and strains on components and materials. We have only one camera meanwhile and we can perform measurements only on planar samples. Thus a modified device of Arcan (1978) was constructed capable of providing uniform plane stress in the central area of a butterfly specimen at Fig.7. A distribution of Green shear strain Exy in the Arcan specimen determined by Q400 correlation system and the Istra software is at Fig. 8.

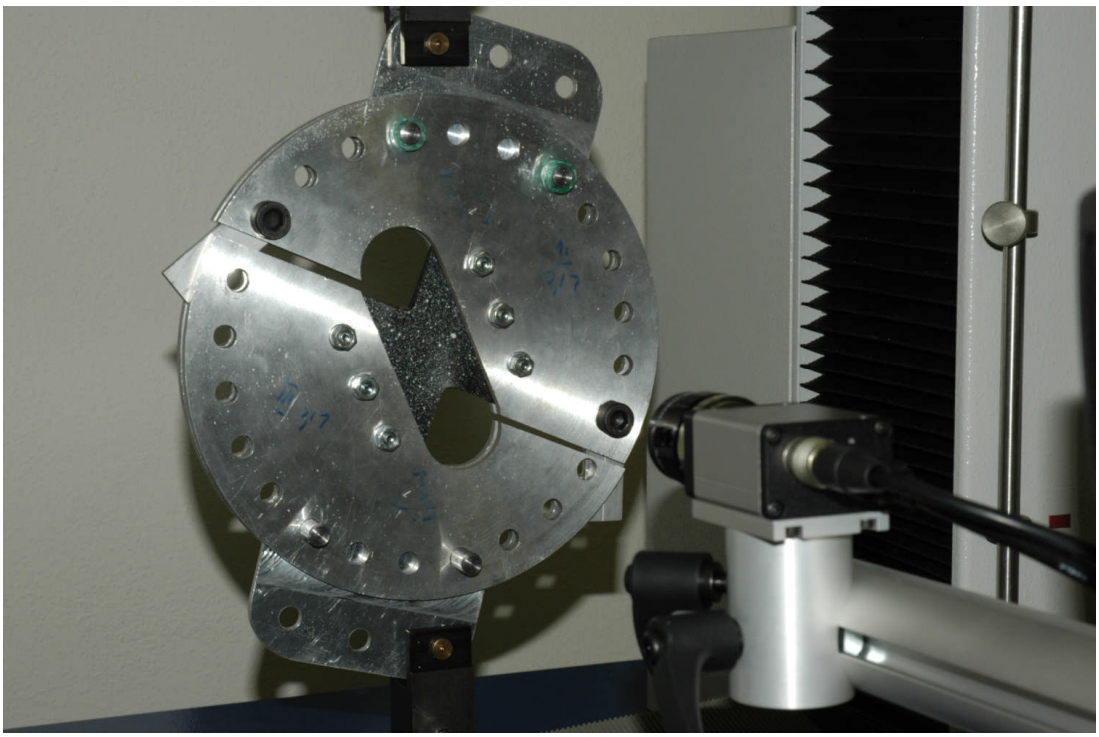

Fig.7. Modified Arcan device and Dantec Q400 system camera
7. ábra Módosított Arcan berendezés és a Dantec Q400 rendszer kamera

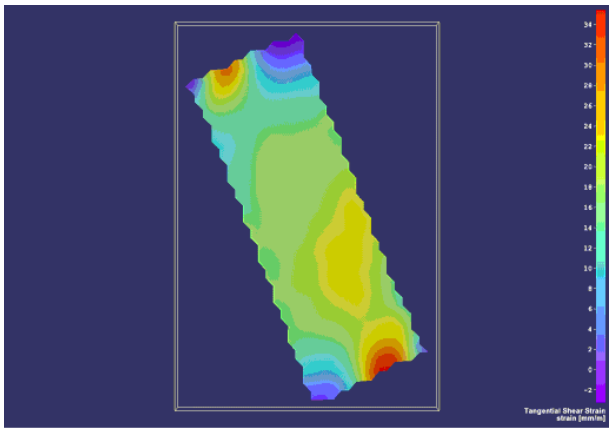

Fig.8. Tangential shear strain in Arcan butterfly specimen
8. ábra Tangenciális csúsztató nyúlás az Arcan féle pillangó próbatestben

Verification of material model – numerical simulations

The orthotropic composite model of the material with the rubber matrix reinforced by textile cords was incorporated into the FEM analysis of the large deformations of the inflated cylindrical air-spring. The axisymetric membrane element kinematics and the constitutive equations were developed. The tangent stiffness matrix and the external force vector were also formulated. The computation in Matlab was carried out by Tran Huu Nam (2004). Intermediate stages of inflated membrane and limit points were computed by the combination of modified Newton-Raphson method with load increments controlled by the iteration count of previous convergence and by the arc-length method. Another model based on rebar elements at Fig. 9 was implemented in ANSYS by Urban (2005). Different hyperelastic anisotropic material models were implemented into Comsol Multiphysics by Hoang Sy Tuan (2007). This FE code allows largely the user implementation of different material models.

Conclusion

The overall objective of rubber composite designing is to produce an optimal product with predictable and reliable behavior in service. To achieve this, it is necessary to identify and evaluate the effects of the various material parameters and to determine material characterization under quasi-static, fatigue and environmental loading conditions. An overview of recent advances in the theoretical and experimental research of behaviour of composites with rubber matrix reinforced by textile cords at Technical University of Liberec was reported. The effects of the cord reinforcement on the elastic properties of rubber composite components are investigated. A model is presented for the prediction of the rubber composite material behaviour. Hyperelastic material properties are determined on the basis of experimental measurements. The verification of material models by the comparison of experimental measurements with numerical simulations in finite element code shows good agreement.

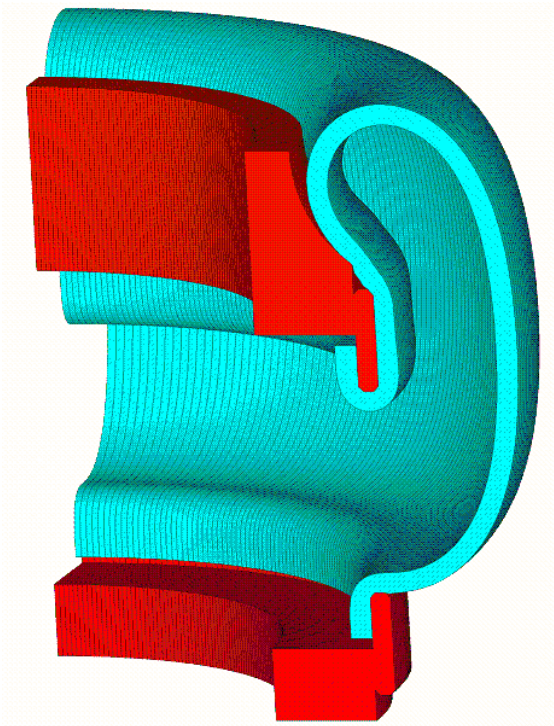

Fig.9. Deformation of a cylindrical air-spring calculated in ANSYS code
9. ábra. A légrugó ANSYS kóddal számított deformációja

Acknowledgement

This work was supported by the subvention from Ministry of Education of the Czech Republic under Contract Code MSM 4674788501

References

1. Arcan, M., Hashin, Z., Woloshin, A., (1978) A Method to Produce Uniform Plane-Stress States with Application to Fiber-Reinforced Materials, Exper. Mech., 18, pp. 141-146.

2. Bouguet J. Y., (2004), Camera Calibration Toolbox for Matlab,
3. http://www.vision.caltech.edu/bouguetj/calib_doc/index.html

4. Garcia D., Orteu J.J., Penazzi L., (2002) A combined temporal tracking and stereo-correlation technique for accurate measurement of 3D displacements: application to sheet metal forming, Journal of Materials Processing Technology, Vol. 125–126, pp. 736–742.

5. Green, A.E., Adkins, J.E., (1965) Bolšije uprugije deformaciji i nelinejnaja mechanika splošnoj sredy, Moskva, Mir.
6. Hoang Sy Tuan, Marvalova, B., (2007) FE analysis of cord-reinforced rubber composites at finite strains, Sb. Výpočty konstrukcí metodou konečných prvků 2007, CVUT Praha, pp. 9-20, ISBN 978-80-01-03942-7

7. Holzapfel G.A., Gasser T.C., Ogden R.W., (2000), A new constitutive framework for arterial wall mechanics and a comparative study of material models, Journal of Elasticity 61, 1-48.

8. Lyons, J. S., Liu, J. & Sutton, M. A., (1996) High-temperature deformation measurements using digital-image correlation, Experimental Mechanics, Volume 36, No 1, pp. 64-70

9. Marvalova, B., Urban, R., (2001) Determination of orthotropic hyperelastic material properties of cord-rubber, Proc. of Euromech colloquium 430, J. Plesek ed., pp.197-198

10. Marvalova, B., Nam, T.H., (2003), Deformation analysis of an inflated cylindrical membrane of composite with rubber matrix reinforced by textile material cords, proc. int. conference Engineering mechanics 2003, Svratka, Czech Republic, pp. 194-195

11. Nam T.H., Marvalova B., (2004) Deformation analysis of inflated cylindrical membrane of composite with rubber matrix reinforced by cords, XXI Int. Congr. Theor. Appl. Mech. ICTAM 2004, Warsaw, ISBN 83-89697-01-1

12. Urban, R., Marvalová, B., (2004) Výpočet deformace pláště válcové pneumatické pružiny. Inženýrská mechanika 2005, Svratka, Eds: V. Fuis, P. Krejčí, P. Švancara, ISBN: 80-85918-93-5, 2005